Transonic Inviscid Flow over Lifting Airfoils by the Method of Integral Relations

TSZE CHENG TAI*
Naval Ship Research and Development Center, Bethesda, Md.

Full inviscid flow equations were employed in a numerical procedure for determining inviscid supercritical flow over prescribed lifting airfoils. Transverse flow variables were approximated by a number of second-order polynomials in accordance with the newly developed multiple-strip arrangement. The effects of shock angle as well as entropy change across the shock wave were evaluated. Five iteration processes were required to solve the subject two-point boundary value problems in a physical plane. The results obtained for various airfoils (two conventional, one advanced, and two shockless) under supercritical flow conditions were in good agreement with available experimental and theoretical data.

Nomenclature

c_v = specific heat at constant volume
K = $1/(\gamma M_\infty^2)$
M = Mach number
N = number of effective regions
$\bar{N}$ = number of strips
P = static pressure normalized by its freestream value
S = specific entropy
$S.L.$ = shock location
s, n = orthogonal curvilinear coordinates measured along and normal to the airfoil surface normalized by the chord length
u, v = velocity components in Cartesian coordinates, normalized by the freestream velocity
V_s, V_n = velocity components along and normal to the airfoil surface, normalized by the freestream velocity
x, y = Cartesian coordinates normalized by the chord length
α = angle of attack
β = oblique shock angle
γ = specific heat ratio
δ = normal distance between the airfoil surface and system boundary normalized by the chord length
θ = inclination with respect to the direction of freestream velocity
ρ = static density normalized by its freestream value

Subscripts
b = at airfoil surface
0 = at base strip boundary, i.e., at streamline passing airfoil surface
1, 2 = before and after shock wave
∞ = freestream

Introduction

THE current research on transonic flows has been phenomenal as reflected by the number of survey and/or review papers that have appeared in the last two years. The Newman-Allison survey[1] lists a great many theoretical papers relating to steady inviscid external transonic flows and provides up-to-date information for assessing the state-of-the-art. Four review papers have recently been published on theoretical methods in transonic flows.[2-5] Those by Norstrud[3] and Wu and Aoyama[5] summarize available analytical and numerical methods for the solution of an appropriate transonic flow problem and cover a broad range of transonic flows. In contrast, those by Murman[2] and Yoshihara[4] are more or less confined to the area of computational methods. The former treats existing methods for flows with embedded shock waves, and the latter is concerned with the hodograph method for shockless flows and finite-difference schemes for more general flows. Both papers emphasize methods based on the use of finite-difference procedures. Papers by Magnus and Yoshihara,[6] Murman and Cole,[7] and Steger and Lomax[8] typify the use of these procedures.

The method of integral relations provides another avenue to the solution of transonic flow problems. In addition to the present work, other recent applications of the method to transonic flows past airfoils include those by Holt and Masson,[9] Melnik and Ives,[10] Sato,[11] and Tai[12] for various flow conditions in transonic regime. In the present paper, a numerical procedure has been developed for calculating transonic flows over lifting airfoils. The use of full inviscid nonisentropic equations allows an entropy change across the shock wave. The procedure is applied to two conventional airfoils, two shockless airfoils, and one advanced (supercritical) airfoil, all at supercritical flow conditions.

Basic Flow Equations

The partial differential equations that govern a steady, adiabatic inviscid fluid flow can be written in a Cartesian coordinate system as follows:

Continuity:

$$\partial(\rho u)/\partial x + \partial(\rho v)/\partial y = 0 \tag{1}$$

x-Momentum:

$$(\partial/\partial x)(KP + \rho u^2) + (\partial/\partial y)(\rho uv) = 0 \tag{2}$$

y-Momentum:

$$(\partial/\partial x)(\rho uv) + (\partial/\partial y)(KP + \rho v^2) = 0 \tag{3}$$

The boundary conditions are as follows: at the airfoil surface, the normal velocity component is equal to zero, i.e.,

$$V_n = u \sin\theta + v \cos\theta = 0 \tag{4a}$$

at infinity, the flow is undisturbed, i.e.,

$$P = \rho = u = 1$$
$$v = 0 \tag{4b}$$

One more equation is needed in order to determine the four dependent variables u, v, ρ, and P, namely, the isentropic relation between the density and static pressure

$$P = \rho^\gamma \tag{5a}$$

This is good for regions prior to the shock wave and the far field. For regions following the shock wave, where the fluid has a finite increase in entropy (or a decrease in the total pressure), the isentropic relation applies along a streamline

Presented as Paper 73-658 at the AIAA 6th Fluid and Plasma Dynamics Conference, Palm Springs, Calif., July 16–18, 1973; submitted August 3, 1973; revision received December 17, 1973. This research was supported by the Naval Air Systems Command (AIR-320) under NAVAIR TASK R230.201. The author wishes to thank H. R. Chaplin, Jr. for his interest and support, S. de los Santos for his valuable suggestions and encouragement and M. Holt of the University of California, Berkeley, for his useful comments.

Index categories: Subsonic and Transonic Flow; Aircraft Aerodynamics (Including Component Aerodynamics).

* Aerospace Engineer, Aviation and Surface Effects Department. Member AIAA.

$$P = \rho^{\gamma} \exp[(S_2 - S_1)/c_v] \tag{5b}$$

The change of entropy $(S_2 - S_1)$ is normally small for transonic flows. However (as will be discussed later) because of the corresponding change of the downstream conditions, it may influence the location of the shock wave and thus alter considerable portions of the entire flow. Nonetheless, the flow behind the shock wave is still isentropic along a streamline which serves as a strip boundary. The new isentropic relation, however, is based on a new entropy level which is slightly higher than its freestream value. The new entropy level differs from one streamline to another because the shock strength encountered on each streamline differs.

The value of the new entropy level is obtained in terms of the static pressure and density immediately after the shock

$$S_2 - S_1 = c_v \ln(P_2/\rho_2^{\gamma}) \tag{6}$$

For an inviscid flow, the shock must be normal at the surface in order to keep the flow attached. The Rankine-Hugoniot relations for normal shock waves are applied here for determining ρ_2 and P_2. They are

$$\rho_2 = \rho_1(\gamma+1)M_1^2/[(\gamma-1)M_1^2+2] \tag{7a}$$

$$P_2 = P_1[1+2\gamma(M_1^2-1)/(\gamma+1)] \tag{7b}$$

Subscripts 1 and 2, respectively, denote values in front of and behind the shock wave.

It is well known that the shock is curved away from the surface. Therefore, the oblique shock relations must be used for the intermediate strip boundary.

$$\rho_2 = \rho_1(\gamma+1)(M_1 \sin\beta)^2/[(\gamma-1)(M_1 \sin\beta)^2+2] \tag{8a}$$

$$P_2 = P_1[1+2\gamma(M_1^2 \sin^2\beta-1)/(\gamma+1)] \tag{8b}$$

where β is the shock angle with respect to the local streamline direction. When $\beta = 90°$, Eqs. (8) become the normal shock relations.

The use of the normal shock relations at the foot of the shock wave is known to be questionable. Emmons[13] found that the Rankine-Hugonoit relations lead to infinite curvature where the shock touches the curved wall of the airfoil. Sichel[14] proposed a model which accounts for the non-Rankine-Hugoniot nature of weak shocks near the wall. The Sichel model includes a viscosity term to give a system of viscous transonic equations for the non-Rankine-Hugoniot region. It is difficult to solve these equations mathematically; but it has been demonstrated that an oblique shock wave represents an exact similarity solution.

On the basis of the preceding arguments, therefore, the normal shock value for the shock jump condition at the foot of the shock could be in great error for certain cases. In such cases, an oblique shock jump should correlate the flow better than the normal shock jump.[15] The angle of the oblique shock, of course, cannot be resolved without considering the viscous-inviscid interaction. An empirical curve of the pressure ratio before and after the shock foot was determined by Sinnot.[16]

In order to be consistent with the inviscid model, the Rankine-Hugoniot relations are applied in the present study at the foot of the shock wave. In some cases, options of oblique shock values are also provided with the shock angle as a free parameter. After the shock wave, the decrease in total pressure is set to zero for cases labelled with $\Delta S = 0$ or takes on a Rankine-Hugoniot value for cases with $\Delta S > 0$.

Numerical Algorithm

Method of Integral Relations (MIR)

The feasibility of applying the method of integral relations to supercritical flows over symmetric airfoils at zero angle of attack has already been studied and demonstrated previously.[12] The approach is now extended to lifting cases.

Briefly, in applying the method of integral relations, the system of flow equations must be written in divergence form

$$\frac{\partial}{\partial x}A(x, y, u, \ldots) + \frac{\partial}{\partial y}B(x, y, u, \ldots) = Q(x, y, u, \ldots) \tag{9}$$

The divergence form of Eqs. (1–3) may then be integrated outward from the airfoil surface (but not necessarily normal to the surface) to each strip boundary successively at some x station. This procedure reduces the partial differential equations to ordinary ones. In order to perform the integration, the variation of integrand along y must be known. A general approach is to approximate the integrands by interpolation polynomials, for example, A by

$$A = \sum_{k=0}^{\bar{N}} a_k(x)(y-y_0)^k \tag{10}$$

where $\bar{N}$ is the number of strips, $a_k(x)$ are constants evaluated at strip boundaries and y_0 is the location of the base strip boundary. In principle, the actual flow variation may be represented more closely by an increasing number of strips.

The ordinary differential equations derived by using a second-order polynomial were presented in the earlier work.[12] For use in the lifting case, however, they are applied separately for both upper and lower flowfields. The division of the flowfields will be discussed later.

In order to examine the higher order effect in the MIR, a set of ordinary differential equations is derived by using a regular third-order polynomial. The system was coded first for the computation of upstream flow. The third-order equations were found less stable than second-order ones. The instability is attributed to the generation of a negative value of dv/dx in the first few steps of integration in the upstream region. This negative dv/dx is contradictory to the physical phenomenon and entirely caused by the mathematical inflection point of the third-order polynomial. Not every third-order polynomial has an inflection point, but one easily becomes inflected if it represents a transverse flow variation from the undisturbed state. Possibly it would have worked better than the second-order equations in other flow regions; but in any event, the computation has to start from the upstream region. Complexity is another unpleasant feature of third-order equations. For these reasons, they are no longer employed.

Coordinate Systems

Cartesian coordinates are employed as the basic coordinates. In the region of the leading edge where drastic changes of body slopes are involved, a body-oriented orthogonal curvilinear coordinate system is incorporated. The latter is embedded in the former, see Fig. 1. The solution of the outer region interacts with that for the inner region. Since the width of the inner region is normally fairly thin, one-strip approximation is used in this region. Ordinary differential equations by using a one-strip approximation in the orthogonal curvilinear coordinates were obtained earlier.[12] The system is now revised by the addition of a momentum equation to account for the effect of body properties on the outer flow. The present forms have already been given in Ref. 17.

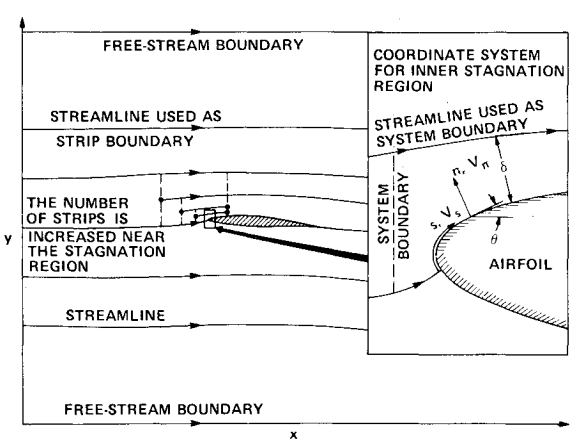

Fig. 1 Coordinate systems and strip boundaries.

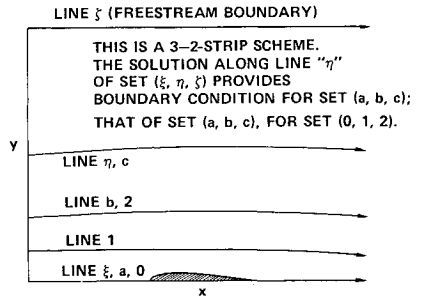

Fig. 2 Extension of freestream boundary to "infinity."

There are two reasons for using the preceding coordinate systems in the physical plane. First, the method of integral relations is a universal numerical method. If no particular advantage can be secured by using any sophisticated transformation, convenience should surely prevail, particularly when modern high-speed computers are available. Second, where calculations of supercritical flows involve mixed elliptic-hyperbolic flow characters, it is difficult to select a function as a basis of transformation to a computational plane. For example, functions based on incompressible solution such as used by Chushkin[18-20] become highly inadequate in the present case.

When a closed form is not available for airfoil coordinates, the geometry of the airfoil is represented by cubic spline functions.[21]

Strip Boundaries and Division of Flowfield

Even though no transformation of coordinates is involved, the freestream boundary can still be set at "infinity" in the present study. This is implemented by a new arrangement of strip boundaries. As shown in Fig. 2, the idea is to treat the whole integration domain as a series of different effective regions; a small number of strips may be used within each region. For simplicity, only the upper part of a symmetric airfoil is shown. Three effective regions are designated by strip boundaries (0, 1, 2), (a, b, c), and (ξ, η, ζ). In each effective region, the flowfield is divided into two strips and approximated in the usual way by a second-order polynomial. For strips with lines (0, 1, 2), the solution may be integrated if the flow properties along line "2" are given. If line "2" coincides with *"b"* of set (a, b, c), then the boundary conditions along line "2" are determined by integration along line *"b"* with another two-strip approximation for lines (a, b, c). Similarly, the values along line *"c"* are provided by results along line *"η"* obtained from integration of lines (ξ, η, ζ). The integration of all sets should be carried out simultaneously with a single-valued solution along each line. The procedure may be repeated many times to extend the final freestream boundary at "infinity."

The new arrangement is called N-2-strip integration scheme; whereas $N = 3$ in Fig. 2. The total number of strips will be $N+1$. It allows the use of a large number of strips without need for the higher order polynomials which usually cause numerical difficulties in actual computation. For instance, the solution for the four-strip flowfield in Fig. 2 employs three sets of second-order polynomials instead of one set of fourth-order polynomials.

In the present approach, some typical streamlines are used as strip boundaries. The upper and lower flowfields are divided by the streamline passing along the airfoil surface. In the upstream region, this streamline is called the stagnation streamline. On reaching the stagnation point, it splits into the upper and lower surfaces of the airfoil and meets again at the trailing edge. After leaving the trailing edge, it flattens out and asymptotically approaches an undisturbed state far downstream. The equations for determining the stagnation streamline geometry are derived by using a procedure similar to that presented in Ref. 22.

Five strips are used in the far field of the upstream region and eight in the near field of this region for both upper and lower sides. Six strips are employed for the leading edge region including the strip associated with the orthogonal curvilinear coordinates. The number may be reduced to five if the sonic line touches the nearest strip boundary. Depending on the flow condition or the local airfoil curvature, four or five strips are generally used for the airfoil region; the number can even be decreased to three in the downstream region. The freestream boundary is set about seven chord lengths away from the airfoil. The preceding strip arrangement represents somewhat of a compromise between accuracy and numerical instability. An important factor for the setup, of course, is that it allows the recovery of the freestream values in the far downstream for the sake of existence and uniqueness of the solution. The schematic view of the strip arrangement is shown in Fig. 1.

Numerical Integration

With the partial differential equations reduced to a set of ordinary differential equations by the method of integral relations, the numerical integrations were carried out along the longitudinal axis x by using a standard fourth-order Runge-Kutta method. A complete solution involves five iteration processes as discussed in the next section. The details of the integration have been described in Ref. 17.

A typical converged run on a CDC 6700 computer requires a storage capacity of about 14,000 and an average of 0.04 sec per step size for various strip arrangements. In all, 700 to 1000 steps are needed for integration from upstream to downstream. This amounts to about 30–40 sec for a converged run. To account for the necessary iterations, some parts of the previous figure have to be increased 30 to 90 times. Thus, the total computation time will be somewhat between 15 to 50 min. Now that the program has been improved and incorporated with an interactive graphics system, it requires about 5 to 10 min for a typical case.

Two-Point Boundary Value Problem—Iterations

Mathematically, transonic flow past an airfoil constitutes a boundary value problem. When the governing partial differential equations are reduced to an ordinary set by some means (such as the method of integral relations in the present study), the problem becomes a two-point boundary value problem. The general strategy for solving the subject problem is the so-called initial value technique wherein initial values for the integration are estimated and iterated from time to time until the imposed or terminal conditions are satisfied. The complete solution procedure consists of five iteration processes which are illustrated in Fig. 3 and described below.

Iteration I—Upstream Integration

The upstream flow is influenced by the presence of the airfoil. The iteration process here is concerned with the feedback of the geometric and flow properties in the stagnation region to the upstream flow. The variation of the upstream flow initially

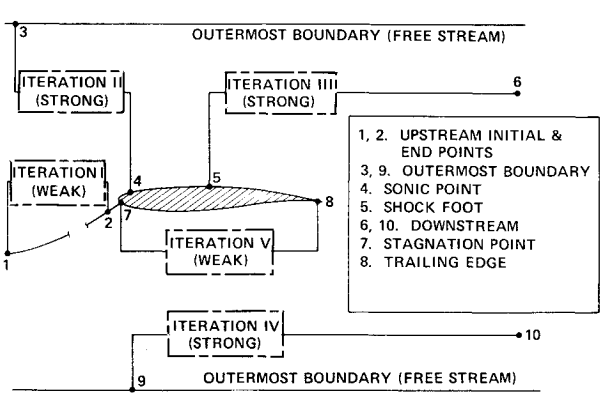

Fig. 3 Iteration procedures for solving subject two-point boundary value problems.

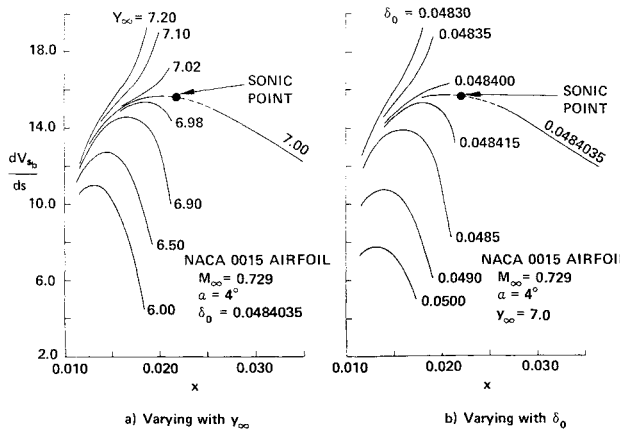

Fig. 4 Velocity gradients near sonic point.

starts through an artificial disturbance. The form of the disturbance was assumed initially and subsequently improved through successive integrations. Since the disturbance is applied only for the first several steps in the upstream integration, rapid convergence is obtained. The iteration has only a slight effect on the final result. Thus it is a weak iteration.

Iteration II—Treatment of Sonic Point

For supercritical flows, the ordinary differential equations have at least one saddle-type singularity at the sonic critical point (or near the sonic point if the equations are written in Cartesian coordinates) where the denominator goes to zero when $M = 1$. Physically, however, there should be a continuous flow through the sonic point(s). A continuous solution exists only if the numerator and denominator of that equation simultaneously become zero so that the ratio 0/0 still yields a finite quantity. In order to force the numerator to zero when $M \to 1$, adjustment of certain unknown parameter(s) in the course of the solution is mandatory. The present iteration, therefore, adjusts certain unknown parameters so that a continuous solution exists at the sonic point.

The height of the outermost strip boundary y_∞ was used as the varying parameter. It was introduced to modify the original infinite integration domain to a finite one. Since all the strips change in thickness as the boundary is moved, there is a direct effect on the initial condition as well as on the flowfield. First, the outermost boundary is approximately set in accordance with a specific strip arrangement and the strip spacings are defined as fractions of the quantity y_∞. Integration then proceeds and the solution generally diverges as it approaches the critical point. The value of y_∞ is then perturbed† and integration repeated. The converged solution is obtained by determining the quantity y_∞ such that the value of the surface velocity gradient immediately aft of the critical point coincides with that extrapolated through the critical point. The idea is analogous to the hypersonic blunt body problem in which the adjustment of the shock standoff distance is required for a continuous solution through the sonic point.

In fact, the abovementioned procedure eventually absorbs all the constituents of the inaccuracies in the initial conditions, i.e., polynomial approximation, strip arrangement, numerical truncation, approximated values for some physical parameters, and so forth. If one of the preceding sources of inaccuracy is changed, the varying parameter has to be adjusted over again. Thus, determination of the unknown parameter is based on a combination of fixed values for all other extraneous and physical parameters. This procedure is similar to that described by Klineberg et al.[23] in connection with the provision of unique initial conditions by requiring the correct "trajectory" to pass through the critical point. It is therefore equally valid if another parameter is used as the varying parameter and the others, including the outermost boundary location, are fixed. The outermost boundary location is then approximately set by consideration of the accuracy of the solution.

An alternative parameter is δ_0, the distance between the end station of the upstream region and the stagnation point. Its value has a direct effect on the velocity gradient at the stagnation point. In this case the approximate value δ_0 is then adjusted such that a continuous solution exists at the sonic point. Although the outermost boundary location was used as the varying parameter in all practical computations for the present work, it is demonstrated that the distance δ_0 can be employed as the varying parameter as well. Figure 4 shows the behavior of the surface velocity gradients near the sonic critical point when the quantities y_∞ and δ_0 are used in turn as the varying parameter. It is clearly seen that the end effects of both options is the same. The results indicate that it is appropriate to utilize these two parameters simultaneously as the varying parameters for handling cases where the sonic line crosses an intermediate strip boundary as well as the surface boundary. This kind of situation might occur under some extreme flow conditions.

The iteration has a marked effect on the final result. Thus, it is a strong iteration.

Iteration III—Determination of Shock Location

The procedure for determining the shock wave location was based on the hypothesis that the shock wave location is determined by the condition whereby the flow returns to its undisturbed state sufficiently far downstream. It is analogous to the principle of nozzle flow where the location of the shock is determined by matching the static pressure at the nozzle exit. In lifting cases, however, the downstream condition is checked separately for both upper and lower regions.

During the iteration process, the Rankine-Hugoniot relations are applied at a number of assumed shock foot locations. After the shock wave, the integration resumes down to the trailing edge and finally through the downstream region. The results for each assumed shock location are then checked to determine whether the downstream boundary condition is satisfied, i.e., whether the flow based on a particular shock location approaches a uniform state in the far downstream. The shock location that meets this criterion is considered "correct" and the others "wrong."

In practical computations, however, a complete uniform flow cannot be obtained because of accumulated numerical errors. Under these circumstances, a general approach is to consider that the solution is satisfactory when the uniform flow value can be bracketed by two integral curves based on two shock locations. This is shown in Fig. 5 where typical pressure distributions along the $y \cong 0$ strip boundary for the upper region are plotted for various assumed shock locations for an NACA 0015 airfoil at $M_\infty = 0.729$ and $\alpha = 4°$. Attention is given to the curves based on shock locations at $x = 0.50$ and 0.51. Although the difference in the shock locations is minimal, the difference in the resulting pressures is not. It is observed that the freestream value is

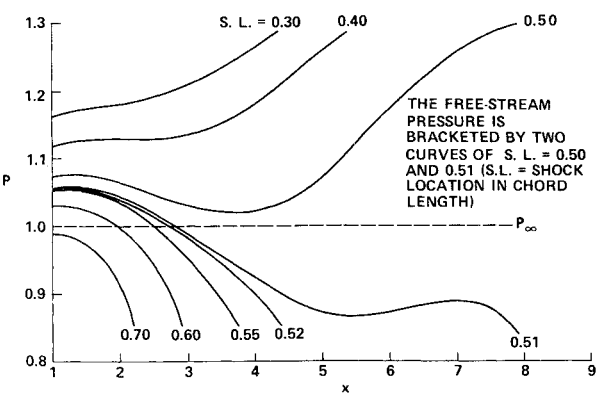

Fig. 5 Downstream pressure distribution on $y \cong 0$ streamline for a NACA 0015 airfoil at $M_\infty = 0.729$ and $\alpha = 4°$.

† The thickness of all strips is perturbed proportionally. If all strips are fixed, the result is very insensitive to the changes in y_∞.

bracketed in these two sets of curves. It is also interesting to note that the freestream pressure is bracketed not only along the $y \cong 0$ boundary but also along other intermediate strip boundaries.[17] The results imply that the downstream boundary condition is satisfied for all the strips. The shock location determined by the present procedure is also unique within the framework of the method. This is supported by the fact that a wide range of shock locations is covered in Fig. 5. The actual shock location therefore lies somewhere between $x = 0.50$ and 0.51.

The principle behind the present iteration is that satisfaction of the downstream flow condition implies a downstream influence on the entire flow. The downstream influence propagates to the upstream throughout the whole flowfield in subcritical flows (see Iteration IV). In a supercritical flow, however, part of the influence propagates up to and stops at the shock wave because the embedded supersonic region in front prevents the propagation of any influence to the upstream. In fact, since it is close to the surface, this part of the influence contributes the major portion of the downstream feedback. That is why the downstream flow is so closely affected by shock wave location. The other part of the influence propagates to the upstream through the intermediate strips where the flow is subcritical. The upstream flow is affected by this part of the influence through Iteration II.

Iteration IV—Integration for Subcritical Flow

The iteration developed here for the integration of subcritical flow is based more or less on the ideas used in Iterations II and III. That is, if there is no embedded supersonic region, there will be no sonic critical point and no shock location problem. Therefore, the present iteration is concerned with determining an outermost boundary location that satisfies the downstream boundary condition. During the iteration process, the outermost strip location is adjusted similarly as in Iteration II and the corresponding downstream results are checked as in Iteration III. The freestream value is bracketed in curves with outermost boundary locations at $y_\infty = 7.04$ and 7.06. The result is given in Ref. 17.

The integrations in the downstream region are carried out separately for both upper and lower regions. This independent treatment of the upper and lower flowfields provides a clear indication of the downstream flow trend, and that is important in bracketing the freestream values for each region. In so doing, it seems that the pressure distribution along the $y \cong 0$ strip boundary is multivalued. Actually, however, the pressure distributions obtained along the $y \cong 0$ boundary from either region are merely for the purpose of bracketing freestream values; at most, they can be considered only as neighboring solutions. And by the same token, the bracketed solutions from both the regions are themselves the neighboring solutions. Thus there is no multivalued solution problem. Fortunately there is no need to find the true solution along either strip boundary in the downstream region.

Iteration V—Enforcement of Kutta Condition

The Kutta condition is satisfied by matching the static pressures at the trailing edge from integrations along both the upper and lower surfaces. The stagnation point at the leading edge is changed by utilizing its influence on the initial conditions for both sides. During the iteration process, a stagnation point is assumed somewhere at the leading edge and, consequently, the initial conditions are calculated at respective initial points a small distance away from the assumed stagnation point. The numerical integrations are then carried out along both upper and lower surfaces and the end result at the trailing edge is checked. If the difference in static pressures at both upper and lower sides of the trailing edge exceeds a certain specified tolerance, a new stagnation point is selected. The whole procedure is then repeated until satisfactory matching in pressure at the trailing edge is obtained. For purposes of this matching, the pressure values should be those which satisfy the imposed and downstream boundary conditions. That is, they should be the converged values from Iterations I–IV. Fortunately, if the specified tolerance is not too small, say somewhere between 2% and 3%, the present iteration is easily converged. Inasmuch as it involves the converged values of all previous four iterations, the present iteration therefore provides over-all downstream influence to the upstream region.

The abovementioned procedures are formulated for flow conditions where the shock wave does not touch the boundary of the strip adjacent to the airfoil. This boundary is usually set between 0.7 to 0.9 chord length to allow a full development of the local supersonic flow. In fact, the present size of the supersonic pocket covers almost all supercritical flows of practical interests, including an important class of general transonic flows considered in existing methods,[6–13] all the shockless flows,[24–29] and known experimental measurements as well.[28,30–32] The physical boundary has even less restraint on the strength of the shock wave since the latter depends on how favorably the supersonic flow is developed[32] rather than on the size of the embedded supersonic region. In any case, the numerical results indicate that the present size of the supersonic pocket is more than adequate to permit studying the basic features of a supercritical flow, including the effect of entropy change across the shock wave.

The method can be readily extended to cases with extreme flow conditions in which the embedded supersonic region may cross more than one strip boundary. It is then necessary to assume the shape of the shock wave in order to locate the proper station to apply the shock relations at the intermediate strip boundary. In addition, more than one varying parameter should be employed for determining the converged solution through the critical points, as discussed in Iteration II. Since the iteration involves only part of the over-all flow calculations, no large increase in computing time is anticipated.

Results and Discussion

Results at supercritical freestream Mach numbers were calculated for two conventional, one advanced (designed for supercritical), and two shockless airfoils. Flow conditions were chosen to enable comparisons with available theoretical and/or experimental data. Since Iterations II, III, and IV are non-negotiable, they were all carried out accordingly. Iterations I and V have been converged to within 2.5%.

Figure 6 represents a comparison of the calculated surface pressure distribution on an NACA 64A410 airfoil at $M_\infty = 0.72$ and $\alpha = 4°$ and those obtained by using the unsteady finite-difference scheme of Magnus and Yoshihara[6] and the experimental data except in the neighborhood of the shock wave. The disagreement there is attributed to a strong interaction between shock wave and boundary layer. The agreement between the present method and the unsteady finite-difference scheme was generally good. In the unsteady finite-difference scheme, however, the pressure jump across the shock wave had to be spread in several steps rather than evaluated by the Rankine-Hugoniot

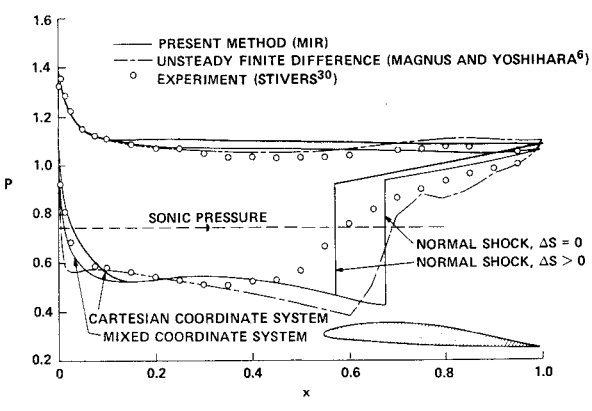

Fig. 6 Pressure distribution on an NACA 64A410 airfoil at $M_\infty = 0.72$ and $\alpha = 4°$.

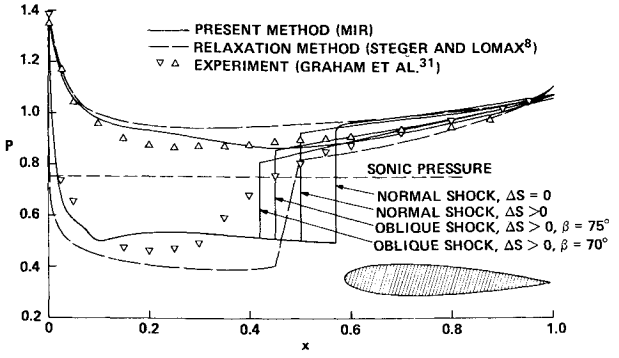

Fig. 7 Pressure distribution on an NACA 0015 airfoil at $M_\infty = 0.729$ and $\alpha = 4°$.

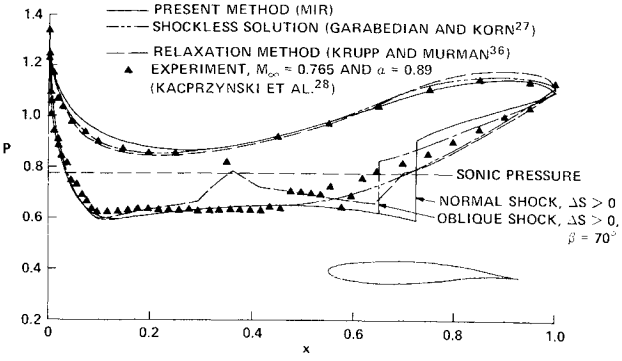

Fig. 9 Pressure distribution on a Garabedian-Korn airfoil at $M_\infty = 0.75$.

relations as employed in the present method. The difference in the surface pressure due to the use of mixed coordinates was noticeable between $x = 0$ to 0.15.

Figure 6 also indicates that if there is an increase in entropy (or a decrease in total pressure) across the shock wave, its location moves forward. This phenomenon qualitatively agrees with nozzle flow in which the shock wave moves upstream in the case of a smaller total pressure.[33] As a consequence, part of the over-all flowfield is altered. Hayes[34] has indicated the problem of a cumulative nonlinear effect of entropy change which grows to first-order over a long distance.

Figure 7 compares the calculated surface pressure distribution on an NACA 0015 airfoil at $M_\infty = 0.729$ and $\alpha = 4°$ with theoretical results obtained by using the relaxation method[8] and with the experimental data of Graham et al.[31]

The present results show that the location of a normal shock wave moves forward in case of a finite entropy change across the shock wave. The trend agrees with that for the NACA 64A410 airfoil, as previously discussed. Furthermore, in the case of an oblique shock, allowing an entropy change across the shock shifts the shock location forward; the smaller the shock angle, the more forward the shock location. The same is expected to be true if there were no entropy change across the shock wave. Ferrari and Tricomi[15] have demonstrated qualitatively that an oblique shock wave occurs earlier than a normal shock wave. Figure 73 of their book compares results of shock-foot locus from the theoretical prediction of Spreiter and Alksne[35] with the empirical correlation and experimental data of Sinnot.[16] The figure indicates consistently that the Sinnot empirical shock locations (which correspond to oblique shocks) for various airfoils were considerably more forward than those obtained by using normal shock values.

The best agreement of results from the present study with experimental data was for oblique shock $\beta = 70°$ and finite entropy change. The smaller the shock angle, the better the correlation. Actually, the experimental data revealed a strong viscous effect near the shock wave. The use of oblique shock options in our formulation, however, has the effect of compensating for viscous effect. Compared with the theoretical predictions of the relaxation method,[8] the present method yielded milder acceleration in the upper leading edge. The two methods were in fair agreement for results on the lower surface of the airfoil.

Figure 8 shows the surface pressure distribution calculated for an advanced airfoil of 17% thickness ratio at $M_\infty = 0.70$ and $\alpha = 1.5°$. A fairly peaky pressure distribution was observed in the leading edge region for the upper surface. Unlike conventional airfoil cases, the pressure increased all the way toward the shock wave after the peak velocity had been reached. The local supersonic flow was therefore favorably developed for reducing the shock strength as suggested by Pearcey.[32] The result for an oblique shock differed little from that for a normal shock because the viscous effect is minimal for very weak shock waves. Moderate acceleration of the flow occurred up to 45% of the chord on the lower surface and was then followed by a strong deceleration zone. The cusp near the trailing edge helped to bring the pressure down to match that of the upper surface.

Figure 9 compares the calculated results on a Garabedian-Korn shockless airfoil at the design condition of $M_\infty = 0.75$ with the original solution of Garabedian and Korn,[27] the small disturbance solution of Krupp and Murman,[36] and the experimental data of Kacprzynski et al.[28] In general, all three theoretical solutions agreed fairly well over most portions of the airfoil surface. After the midchord, the present result started to deviate from the original shockless solution because the flow started to accelerate rather than decelerate. The explanation is that from thereon the surface slopes became negative and corresponded to a divergent local area for two-dimensional flow. Therefore they caused the local supersonic flow to expand and as a consequence of this local expansion, the flow must be brought back to its subsonic state by a shock wave. Here again, both normal and oblique shock relations were applied in the computation. It was observed that the shock location moved forward as its strength decreased from a normal shock to an oblique shock. A further decrease in shock strength would have

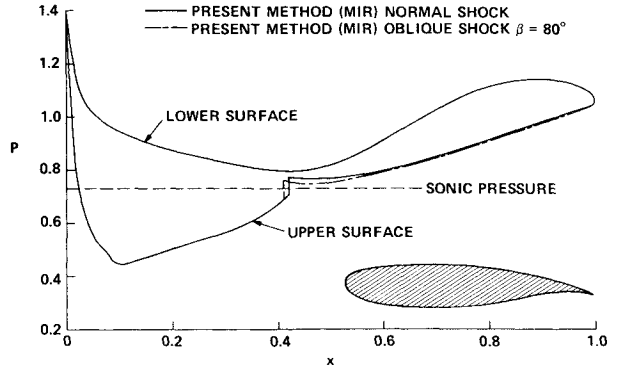

Fig. 8 Pressure distribution on an advanced airfoil of 17% thickness ratio at $M_\infty = 0.70$ and $\alpha = 1.5°$.

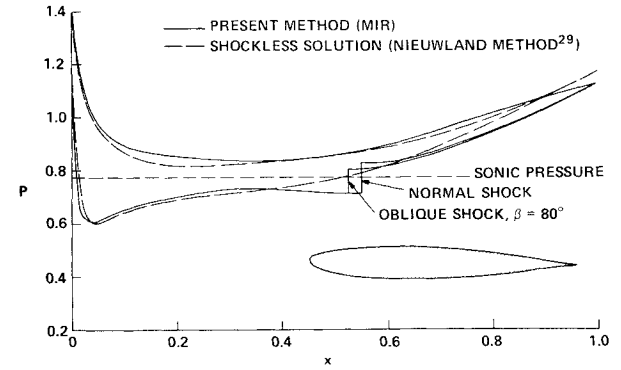

Fig. 10 Pressure distribution on a Nieuwland airfoil at $M_\infty = 0.7557$ and $\alpha = 1.32°$.

resulted in a "shockless condition" as a limit. The experimental data which were measured at slightly different freestream Mach numbers and angles of attack exhibited considerable variation or spread in the compression region. These variations are most likely attributable to a series of weak shocks.

Finally, the results for a quasi-elliptical airfoil by the Nieuwland approach[24] at $M_\infty = 0.7557$ and $\alpha = 1.32°$ are presented in Fig. 10. The original shockless solution tabulated by Lock[29] is also given for purposes of comparison. The agreement between the two solutions was good except for the occurrence of a shock wave in the present result. The explanation for this difference is very much the same as in the case of Garabedian-Korn airfoil. Similar to previous cases, the oblique shock wave simulated the flow better than did the normal shock.

Conclusion

The full inviscid flow equations were employed in the present numerical procedure for determining inviscid supercritical flows over prescribed lifting airfoils. Transverse flow variables were approximated by a number of second-order polynomials in accordance with the newly developed multiple-strip arrangement. Five iteration processes were required to solve the subject two-point boundary value problems in a physical plane.

Calculated results for supercritical flows past various airfoils (two conventional, one advanced, and two shockless) compared fairly well with existing theoretical and/or experimental data. It was found that the shock location moves forward when there is a finite increase in entropy across the shock wave. The correlation between the present theoretical results and experimental data was better when oblique shock rather than normal shock was used. Shock location is shifted forward for an oblique shock; the smaller the shock angle, the more forward the shock location.

The relatively small amount of computer running time involved and the reasonably good accuracy that is obtainable make the present method attractive for analyzing transonic full inviscid flow. Furthermore, because computer storage requirements are small, it is easy to couple the method with viscous analysis for the investigation of transonic shock-wave/boundary-layer interaction problems.

References

[1] Newman, P. A. and Allison, D. O., "An Annotated Bibliography on Transonic Flow Theory," TM X-2363, Sept. 1971, NASA.

[2] Murman, E. M., "Computational Methods for Inviscid Transonic Flows with Imbedded Shock Waves," Document D1-82-1053, Feb. 1971, Boeing Scientific Res. Lab., Seattle, Wash.

[3] Norstrud, H., "A Review of Transonic Flow Theory," Rept. ER-11138(L), Aug. 1971, Lockheed-Georgia Co., Marietta, Ga.

[4] Yoshihara, H., "Some Recent Developments in Planar Inviscid Transonic Airfoil Theory," AGARD AG-156, Feb. 1972.

[5] Wu, J. M. and Aoyama, K., "Preliminary Review of Approximate Calculative Methods for Transonic Flow around Bodies of Revolution," RD-TR-72-4, March 1972, Univ. of Tennessee Space Inst., Tullahoma, Tenn.

[6] Magnus, R. and Yoshihara, H., "Inviscid Transonic Flow over Airfoils," *AIAA Journal*, Vol. 8, No. 12, Dec. 1970, pp. 2157–2162.

[7] Murman, E. M. and Cole, J. D., "Calculation of Plane Steady Transonic Flows," *AIAA Journal*, Vol. 9, No. 1, Jan. 1971, pp. 114–121.

[8] Steger, J. L. and Lomax, H., "Numerical Calculation of Transonic Flow About Two-Dimensional Airfoils by Relaxation Procedures," *AIAA Journal*, Vol. 10, No. 1, Jan. 1972, pp. 49–54.

[9] Holt, M. and Masson, B. S., "The Calculation of High Subsonic Flow Past Bodies by the Method of Integral Relations," *Proceedings of the Second International Conference on Numerical Methods in Fluid Dynamics*, Vol. 8, Springer-Verlag, New York, 1971, pp. 207–214.

[10] Melnik, R. E. and Ives, D. C., "Subcritical Flows of Two-Dimensional Airfoils by a Multistrip Method of Integral Relations," *Proceedings of the Second International Conference on Numerical Methods in Fluid Dynamics*, Vol. 8, Springer-Verlag, New York, 1971, pp. 243–251.

[11] Sato, J., "Application of Dorodnitsyn's Technique to Compressible Two-Dimensional Airfoil Theories at Transonic Speeds," TR-220T, Oct. 1970, National Aerospace Lab., Tokyo, Japan.

[12] Tai, T. C., "Application of the Method of Integral Relations to Transonic Airfoil Problems: Part I—Inviscid Supercritical Flow over Symmetric Airfoil at Zero Angle of Attack," NSRDC Rept. 3424, Sept. 1970, Naval Ship Research and Development Center, Bethesda, Md.; brief version presented as AIAA Paper 71-98, New York, 1971.

[13] Emmons, H. W., "Flow of a Compressible Fluid past a Symmetrical Airfoil in a Wind Tunnel and Free Air," TN 1746, Nov. 1948, NACA.

[14] Sichel, M., "Structure of Weak Non-Hugoniot Shocks," *The Physics of Fluids*, Vol. 6, No. 5, May 1963, pp. 653–662.

[15] Ferrari, C. and Tricomi, F. G., *Transonic Aerodynamics*, translated by R. H. Cramer, Academic Press, New York, 1968.

[16] Sinnot, C. S., "On the Prediction of Mixed Subsonic/Supersonic Pressure Distributions," *Journal of the Aerospace Sciences*, Vol. 27, Oct. 1960, pp. 767–778.

[17] Tai, T. C., "Application of the Method of Integral Relations to Transonic Airfoil Problems: Part II—Inviscid Supercritical Flow about Lifting Airfoils with Embedded Shock Wave," NSRDC Rept. 3424, Pt. II, July 1972, Naval Ship Research and Development Center, Bethesda, Md.

[18] Belotserkovskii, O. M. and Chushkin, P. I., "The Numerical Solution of Problems in Gas Dynamics," *Basic Developments in Fluid Dynamics*, Vol. 1, edited by M. Holt, Academic Press, New York, 1965.

[19] Chushkin, P. I., "Subsonic Flow of a Gas past Ellipses and Ellipsoids," translation of *Vychislitel'naya Maternatika (USSR)*, No. 2, 1957, pp. 20–44.

[20] Chushkin, P. I., "Computation of Supersonic Flow of Gas past Arbitrary Profiles and Bodies of Revolution (The Symmetric Case)," translation of *Vychislitel'naya Maternatika (USSR)*, No. 3, 1958, pp. 99–110.

[21] Ahlberg, J. H., Nilson, E. N., and Walsh, J. L., *The Theory of Splines and Their Applications*, Academic Press, New York, 1967.

[22] Tai, T. C., "Streamline Geometry and Equivalent Radius over a Flat Delta Wing with Cylindrical Leading Edge at an Angle of Attack," NSRDC Rept. 3675, Oct. 1971, Naval Ship Research and Development Center, Bethesda, Md.

[23] Klineberg, J. M., Kubota, T., and Lees, L., "Theory of Exhaust-Plume/Boundary-Layer Interactions at Supersonic Speeds," *AIAA Journal*, Vol. 10, No. 5, May 1972, pp. 581–588.

[24] Nieuwland, G. Y., "Transonic Potential Flow around a Family of Quasi-Elliptical Aerofoil Sections, TR T-172, July 1967, National Aerospace Laboratory, Amsterdam, The Netherlands.

[25] Korn, D. G., "Computation of Shock-Free Transonic Flows for Airfoil Design," NYO-1480-125, Oct. 1969, New York Univ., New York.

[26] Boerstoel, J. W. and Uijlenhoet, R., "Lifting Airfoils with Supercritical Shockless Flow," ICAS Paper 70-15, 7th Congress of the International Council of the Aeronautical Sciences, Sept. 1970, Rome, Italy.

[27] Garabedian, P. R. and Korn, D. G., "Numerical Design of Transonic Airfoils," *Numerical Solution of Partial Differential Equations*, Vol. 2, Academic Press, New York, 1971, pp. 253–271.

[28] Kacprzynski, J. J., Ohman, L. H., Garabedian, P. R., and Korn, D. G., "Analysis of the Flow past a Shockless Lifting Airfoil in Design and Off-Design Conditions," Aero Rept. LR-554, Nov. 1971, National Research Council of Canada, Ottawa, Canada.

[29] Lock, R. C., "Test Cases for Numerical Methods in Two-Dimensional Transonic Flows," AGARD Rept. 575, Nov. 1970.

[30] Stivers, L. S., Jr., "Effects of Subsonic Mach Numbers on the Forces and Pressure Distributions on Four NACA 64A-Series Airfoil Section at Angles of Attack as High as 28°," TN 3162, March 1954, NACA.

[31] Graham, D. J., Nitzberg, G. E., and Olson, R. N., "A Systematic Investigation of Pressure Distribution at High Speeds over Five Representative NACA Low-Drag and Conventional Airfoil Sections," Rept. 832, 1945, NACA.

[32] Pearcey, H. H., "The Aerodynamic Design of Section Shapes for Swept Wings," *Advances in Aeronautical Sciences*, Vol. 3, 1961, Pergamon Press, New York, pp. 277–322.

[33] Liepmann, H. W. and Roshko, A., *Elements of Gas Dynamics*, Wiley, New York, 1957.

[34] Hayes, W. D., "Pseudotransonic Similitude and First Order Wave Structure," *Journal of the Aerospace Sciences*, Vol. 21, No. 11, Nov. 1954, pp. 721–730.

[35] Spreiter, J. R. and Alksne, A. Y., "Thin Airfoil Theory Based on Approximate Solution of the Transonic Flow Equation," Rept. 1359, 1958, NACA.

[36] Krupp, J. A. and Murman, E. M., "Computation of Transonic Flows Past Lifting Airfoils and Slender Bodies," *AIAA Journal*, Vol. 10, No. 7, July 1972, pp. 880–886.